VEGF-A isoforms differentially regulate ATF-2–dependent VCAM-1 gene expression and endothelial–leukocyte interactions

Gareth W. Fearnley[a], Adam F. Odell[a], Antony M. Latham[a], Nadeem A. Mughal[a,b], Alexander F. Bruns[c], Nicholas J. Burgoyne[d], Shervanthi Homer-Vanniasinkam[b], Ian C. Zachary[e], Monica C. Hollstein[f], Stephen B. Wheatcroft[c], and Sreenivasan Ponnambalam[a]

[a]Endothelial Cell Biology Unit, School of Molecular and Cellular Biology, and [c]Division of Cardiovascular and Diabetes Research, Faculty of Medicine and Health, LIGHT Laboratories, University of Leeds, Leeds LS2 9JT, United Kingdom; [b]Leeds Vascular Institute, Leeds General Infirmary, Leeds LS1 3EX, United Kingdom; [d]Fios Genomics, Edinburgh EH16 4UX, United Kingdom; [e]Division of Cardiovascular Biology and Medicine, Rayne Institute, University College London, London, United Kingdom; [f]German Cancer Research Center (DKFZ), 69120 Heidelberg, Germany

ABSTRACT **Vascular endothelial growth factor A (VEGF-A) regulates many aspects of vascular physiology. VEGF-A stimulates signal transduction pathways that modulate endothelial outputs such as cell migration, proliferation, tubulogenesis, and cell–cell interactions. Multiple VEGF-A isoforms exist, but the biological significance of this is unclear. Here we analyzed VEGF-A isoform–specific stimulation of VCAM-1 gene expression, which controls endothelial–leukocyte interactions, and show that this is dependent on both ERK1/2 and activating transcription factor-2 (ATF-2). VEGF-A isoforms showed differential ERK1/2 and p38 MAPK phosphorylation kinetics. A key feature of VEGF-A isoform–specific ERK1/2 activation and nuclear translocation was increased phosphorylation of ATF-2 on threonine residue 71 (T71). Using reverse genetics, we showed ATF-2 to be functionally required for VEGF-A–stimulated endothelial VCAM-1 gene expression. ATF-2 knockdown blocked VEGF-A–stimulated VCAM-1 expression and endothelial–leukocyte interactions. ATF-2 was also required for other endothelial cell outputs, such as cell migration and tubulogenesis. In contrast, VCAM-1 was essential only for promoting endothelial–leukocyte interactions. This work presents a new paradigm for understanding how soluble growth factor isoforms program complex cellular outputs and responses by modulating signal transduction pathways.**

Monitoring Editor
Carl-Henrik Heldin
Ludwig Institute for Cancer Research

Received: May 7, 2014
Revised: Jun 13, 2014
Accepted: Jun 17, 2014

This article was published online ahead of print in MBoC in Press (http://www.molbiolcell.org/cgi/doi/10.1091/mbc.E14-05-0962) on June 25, 2014.

The authors declare no competing financial interests.

Address correspondence to: Sreenivasan Ponnambalam (s.ponnambalam@leeds.ac.uk).

Abbreviations used: Akt, serine/threonine protein kinase c-Akt (protein kinase B); ATF-2, activating transcription factor 2; ERK1/2, extracellular signal-regulated kinase 1 and 2; HL-60, human promyelocytic leukemia cell line; HUVEC, human umbilical vein endothelial cell; NRP1, neuropilin 1; p38 MAPK, 38-kDa stress- and mitogen-activated protein kinase; qRT-PCR, quantitative reverse transcription PCR; siRNA, small interfering RNA; VCAM-1, vascular cell adhesion molecule 1; VEGF, vascular endothelial growth factor; VEGF-A_{121}, VEGF-A isoform 121 residues in length; VEGF-A_{165}, VEGF-A isoform 165 residues in length; VEGFR, vascular endothelial growth factor receptor.

INTRODUCTION

The 58 human receptor tyrosine kinases (RTKs) can be classified into 20 subfamilies, which regulate animal development, health, and disease (Lemmon and Schlessinger, 2010). These type I membrane proteins contain an extracellular ligand-binding domain that "transmits" information through a transmembrane domain to a cytoplasmic tyrosine kinase domain. Ligand binding triggers tyrosine kinase domain activation, with subsequent transautophosphorylation within RTK dimers, recruitment, and phosphorylation of different signal transduction enzymes and substrates. Targeting RTK activity for therapeutic gain is complicated due to the increasing number of soluble and membrane-bound ligands.

Such complexity is exemplified by the vascular endothelial growth factor (VEGF) family. These ligands bind class III RTKs (VEGF receptors 1–3 [VEGFR1–3]) and coreceptors such as neuropilins

Supplemental Material can be found at:
http://www.molbiolcell.org/content/suppl/2014/06/20/mbc.E14-05-0962v1.DC1

(NRPs) NRP1 and NRP2 (Koch *et al.*, 2011). The VEGF-A gene alone encodes seven or more different isoforms that bind VEGFR1 (Flt-1), VEGFR2 (KDR), and neuropilins (Harper and Bates, 2008). VEGF-A gene dose is critical, as heterozygous VEGF-A$^{+/-}$ knockout mouse embryos die during embryogenesis (Carmeliet *et al.*, 1996; Keyt *et al.*, 1996); VEGFR2$^{-/-}$ knockout mice also exhibit embryonic lethality (Shalaby *et al.*, 1995). The most-studied VEGF-A ligand is a mature 165-residue processed polypeptide (VEGF-A_{165}), which promotes endothelial cell survival, proliferation, migration, and angiogenesis. VEGF-A–regulated endothelial responses are especially associated with pathological conditions such as tumor progression (Chung and Ferrara, 2011; Meadows and Hurwitz, 2012).

The binding of VEGF-A to VEGFR2 triggers sustained signal transduction, increased trafficking, and proteolysis (Bruns *et al.*, 2009; Horowitz and Seerapu, 2012; Koch and Claesson-Welsh, 2012; Nakayama and Berger, 2013). A key aspect of VEGF-A–stimulated reprogramming of endothelial cell function is elevated expression of 100–200 genes (Schweighofer *et al.*, 2009; Rivera *et al.*, 2011). VEGF-A–regulated target genes are implicated in a multitude of cellular functions, including cell adhesion, signal transduction, and transcriptional control. A major question concerns the nature of the mechanism(s) that control VEGF-A–stimulated gene expression. Although VEGF-A–stimulated signal transduction via MEK1–extracellular signal-regulated kinase 1 and 2 (ERK1/2), 38-kDa stress- and mitogen-activated protein kinase (p38 MAPK), and JNK pathways could potentially provide multiple means of elevating gene expression, the exact mechanism by which such signal transduction is integrated with nuclear transcriptional control is unclear. One well-known target is the membrane receptor vascular cell adhesion molecule 1 (VCAM-1), whose expression on endothelial cells promotes binding to leukocyte integrin α4β1 (VLA-4), thus promoting endothelial–leukocyte interactions (Jain *et al.*, 1996; Melder *et al.*, 1996). The mechanism underlying this VEGF-A–stimulated gene expression is unclear, with studies suggesting roles for NF-κB (Kim *et al.*, 2001a) and forkhead (Abid *et al.*, 2008) transcription factors in regulating VCAM-1 gene transcription.

A major question is the role of the increasing number of VEGF splice isoforms in regulating vascular and animal function. The human VEGF-A gene alone expresses eight isoforms ranging from 121 to 206 residues in length. One idea is that the VEGF-A gene encodes both proangiogenic and antiangiogenic isoforms that are expressed in different tissues to modulate the vascular response during health and disease (Harper and Bates, 2008). To evaluate the link between VEGF-A–stimulated gene expression and isoform functionality, we investigated VCAM-1 expression. Studies on VEGF-A_{165} and the VEGF-A isoform 121 residues in length (VEGF-A_{121}) showed that these growth factor isoforms differentially activated signal transduction pathways linked to a novel event in the nucleus that regulates VCAM-1 expression.

RESULTS

VEGF-A isoforms differentially regulate VCAM-1 and VEGFR2 turnover and synthesis

The VEGF-A_{165} isoform promotes increased endothelial VCAM-1 expression (Melder *et al.*, 1996; Kim *et al.*, 2001a; Schweighofer *et al.*, 2009). Although the pathway of VEGF-A–VEGFR2 signal transduction is well studied, it is unclear how such events are communicated to the nucleus to control nuclear gene transcription, such as increased VCAM-1 expression (Figure 1A). To investigate this phenomenon, we first asked whether two different VEGF-A isoforms that differ in their carboxy-proximal regions (Figure 1B) caused similar or different effects on VCAM-1 expression levels in primary human endothelial cells (Figure 1C). We first compared VCAM-1 and VEGFR2 levels in endothelial cells stimulated with a maximal stimulatory dose (0.25 nM) of either VEGF-A_{165} or VEGF-A_{121} for 2, 4, 6, 8, and 24 h (Figure 1C). We used endothelial tubulin levels as a control, and such comparisons were used to evaluate varying protein expression in response to VEGF-A stimulation (Figure 1C). Quantification of endothelial VCAM-1 levels revealed a peak of VCAM-1 expression after VEGF-A_{165} stimulation for 8 h corresponding to ~6.5-fold increase compared with the 0 h time point (Figure 1D). This peak in VCAM-1 levels was transient and dropped to ~2.5-fold rise after VEGF-A_{165} stimulation for 24 h (Figure 1D). In comparison, VEGF-A_{121} stimulation failed to significantly elevate VCAM-1 levels (Figure 1C).

VEGFR2 activation leads to transautophosphorylation of multiple tyrosine residues: Y1175 is a key site that undergoes such phosphorylation (Takahashi *et al.*, 2001; Holmqvist *et al.*, 2004; Koch *et al.*, 2011). Monitoring VEGFR2-pY1175 appearance showed that VEGF-A_{165} stimulates rapid and transient phosphorylation of this site, whereas VEGF-A_{121} treatment did not produce significant Y1175 phosphorylation (Figure 1C). VEGF-A-stimulation promotes VEGFR2 ubiquitination, endocytosis, and proteolysis (Ewan *et al.*, 2006). We then asked whether VEGFR2 turnover and synthesis were different upon treatment with either VEGF-A_{165} or VEGF-A_{121} isoform (Figure 1E). VEGF-A_{165} stimulation promoted VEGFR2 degradation over a short time period (2–4 h), with VEGFR2 levels reduced by ~60% after 2 h (Figure 1E). However, VEGFR2 levels returned to baseline after VEGF-A_{165} stimulation for 8 h (Figure 1E). VEGFR2 levels continued on an upward trajectory, with ~50% increase after VEGF-A_{165} stimulation for 24 h (Figure 1E). In contrast, VEGF-A_{121} stimulation appeared to have little effect on VEGFR2 protein levels (Figure 1E). These findings show that two different VEGF-A isoforms have different capabilities in stimulating the turnover and synthesis of not only VEGFR2, but also those of another membrane receptor, VCAM-1.

VEGF-A isoforms differentially regulate multiple signal transduction pathways

VEGF-A stimulates multiple MAPK signal transduction pathways in endothelial cells (Horowitz and Seerapu, 2012; Koch and Claesson-Welsh, 2012), which regulate multiple cellular outcomes (Nakatsu *et al.*, 2003; Karihaloo *et al.*, 2005; Zhang *et al.*, 2008; Xu *et al.*, 2011). In this context, we asked whether the increase in endothelial VCAM-1 levels (Figure 1D) was linked to altered signal transduction pathways activated by the two VEGF-A isoforms, using ligand titration followed by signal transduction pathway analysis (Figure 2). Activation of VEGFR2 and downstream signaling events was first assessed by monitoring transautophosphorylation at cytoplasmic residue Y1175 (Figure 2, A and B). Phosphorylation of Y1175 could be detected within 5 min of stimulation with either VEGF-A_{165} or VEGF-A_{121}, but there were concentration-dependent effects (Figure 2A). Quantification showed that VEGF-A_{121}–stimulated VEGFR2-Y1175 phosphorylation at 0.025 and 0.25 nM was significantly reduced (Figure 3B) in comparison to VEGF-A_{165} (Figure 3A). However, under saturating conditions of VEGF-A (1.25 nM), the peak level of VEGFR2 activation in response to VEGF-A_{165} (Figure 3A) was similar to that induced by VEGF-A_{121} (Figure 3B).

VEGF-A activates ERK1/2, p38 MAPK, and serine/threonine protein kinase c-Akt (Akt; also known as protein kinase B) pathways in endothelial cells (Koch *et al.*, 2011; Koch and Claesson-Welsh, 2012). Both VEGF-A_{165} and VEGF-A_{121} stimulation promoted a rapid and transient peak in ERK1/2 activation within 15 min, with differing magnitudes (Figure 2). Quantification showed that VEGF-A_{121} stimulation resulted in a generally lower level of peak activation

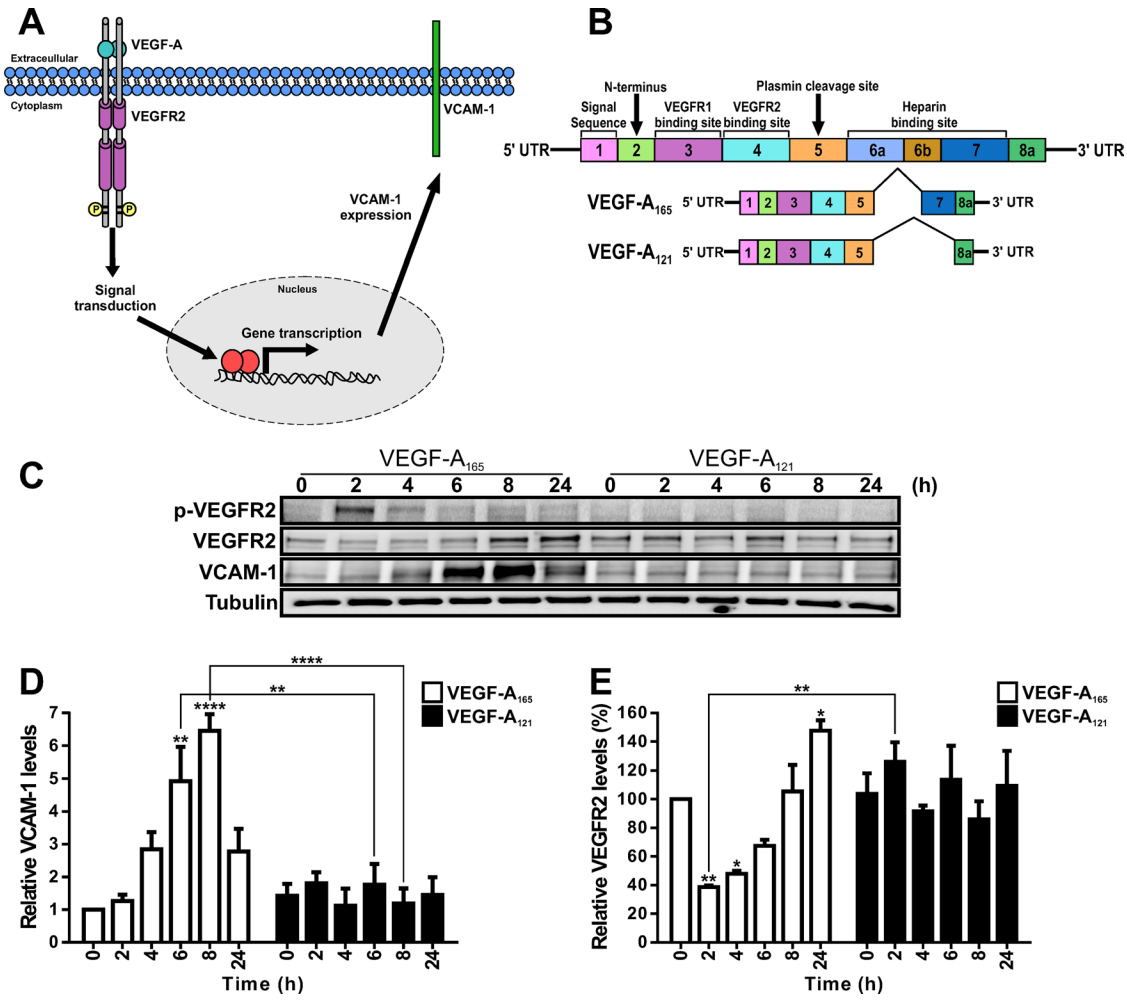

FIGURE 1: VEGF-A isoform–specific regulation of VCAM-1 gene expression. (A) Schematic depicting VEGF-A isoform–specific regulation of VCAM-1 gene expression through modulation of gene transcription in endothelial cells. (B) Schematic depicting human VEGF-A–coding mRNA with exons 1–8 and splice variants VEGF-A_{165} and VEGF-A_{121}. (C) Endothelial cells subjected to 0.25 nM VEGF-A_{165} or VEGF-A_{121} for the specified times indicated (hours), lysed, and probed by immunoblotting to assess phospho-VEGFR2 (VEGFR2-pY1175), VEGFR2, VCAM-1, or tubulin protein levels. (D, E) Quantification of (D) VCAM-1 and (E) VEGFR2 protein levels from immunoblotting studies of VEGF-A_{165}–and VEGF-A_{121}–stimulated endothelial cells. Error bars indicate ±SEM ($n = 3$). *$p < 0.05$, **$p < 0.01$, ****$p < 0.001$.

(Figure 3D) than VEGF-A_{165} (Figure 3C). Of interest, saturating conditions of VEGF-A, which resulted in similar levels of VEGFR2 peak activation (Figure 3, A and B), exhibited approximately twofold difference in ERK1/2 peak activation between the two isoforms (Figure 3, C and D). VEGF-A_{165} and VEGF-A_{121} also triggered sustained and pronounced p38 MAPK activation (Figure 2). Quantification showed that VEGF-A_{121}–stimulated p38 MAPK activation was more pronounced (Figure 3F) than for VEGF-A_{165} (Figure 3E) under saturating ligand conditions. VEGF-A_{165} and VEGF-A_{121} also caused differential Akt activation (Figure 2, A and B). Quantification showed that both VEGF-A_{165} (Figure 3G) and VEGF-A_{121} (Figure 3H) promoted a rapid peak in Akt activation within 15 min. However, VEGF-A_{165} (Figure 3G) had greater efficacy than VEGF-A_{121} (Figure 3H), as a much lower concentration of ligand was required to achieve a significant response. Of interest, at saturating ligand conditions (1.25 nM), the peak in Akt activation was comparable between the two VEGF-A isoforms (Figure 3, G and H). Further analysis of these data sets presented as histograms shows the statistical significance of the changes in signal transduction events detected upon stimulation with either VEGF-A_{165} or VEGF-A_{121} (Supplemental Figure S1). These data suggest that these two different VEGF-A isoforms have differential capabilities not only in stimulating VEGFR2 activation, but also in other downstream signal transduction pathways.

VEGF-A isoform–specific stimulation of activating transcription factor 2

Exactly how short-term RTK signal transduction integrates with long-term cellular responses is not well understood (Lemmon and Schlessinger, 2010). The VEGFR–VEGF-A axis stimulates intracellular signaling over a short time frame (0–1 h) and regulates long-term endothelial responses such as leukocyte recruitment, cell migration (>24 h), and tubulogenesis (5–7 d; Chung and Ferrara, 2011; Koch *et al.*, 2011). To identify a nuclear switch that was responsive to VEGF-A isoform–specific MAPK signal transduction and could influence VCAM-1 expression, we focused on activating transcription factor 2 (ATF-2), which is known to undergo VEGF-A–stimulated phosphorylation in cardiac myocytes and endothelial cells (Seko *et al.*, 1998; Salameh *et al.*, 2010). ATF-2 belongs to the basic region

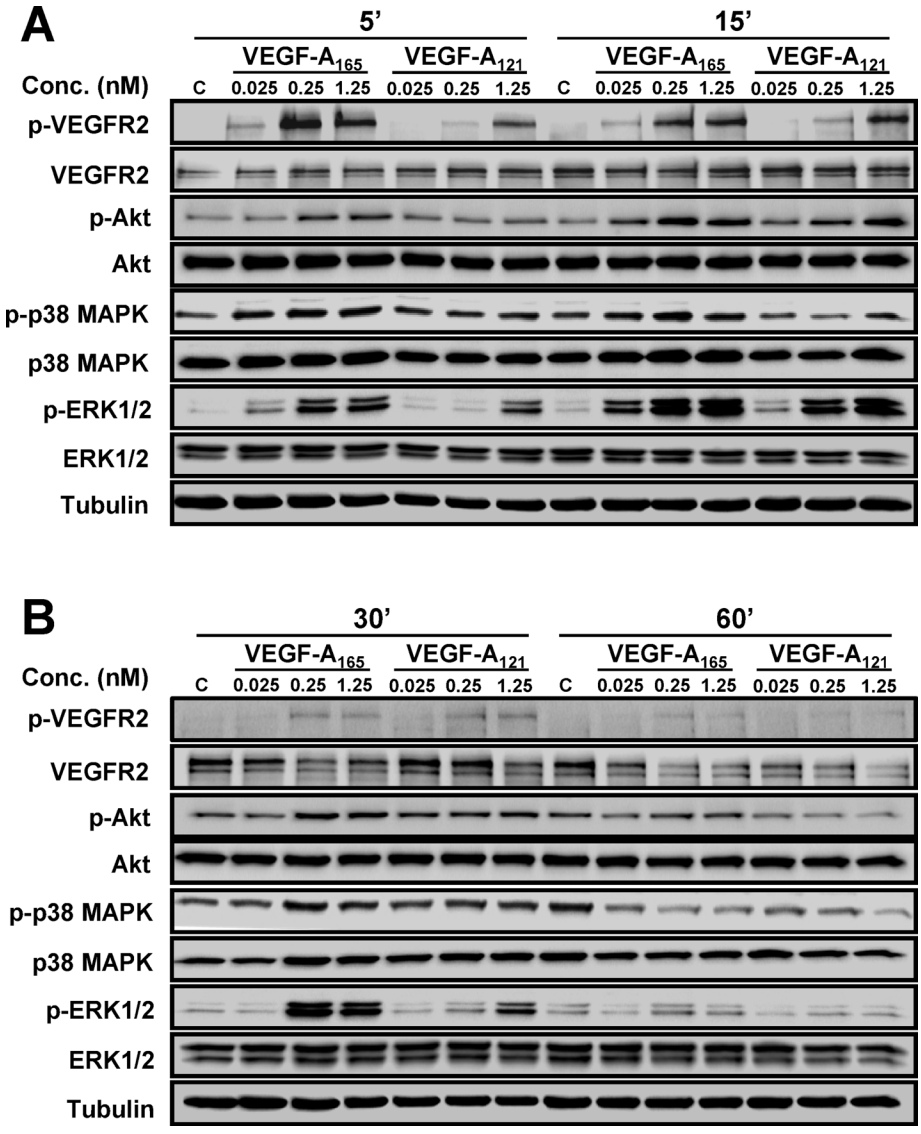

FIGURE 2: VEGF-A isoform–specific activation of signal transduction. (A, B) Endothelial cells subjected to different VEGF-A_{165} or VEGF-A_{121} concentrations (0, 0.025, 0.25, or 1.25 nM) for (A) 5 and 15 min or (B) 30 and 60 min were lysed and probed for phospho-VEGFR2, phospho-ERK1/2, phospho-p38 MAPK, and phospho-Akt (see *Materials and Methods*).

subdomain/leucine zipper (bZIP) family of DNA-binding transcription factors and undergoes activation upon cellular stress or plasma membrane receptor activation (Lau and Ronai, 2012). To determine whether VEGF-A isoforms differentially regulate ATF-2 activation, we monitored ATF-2–pT71 levels (Figure 4A). Endothelial cells contain basal phospho-ATF-2, which is further elevated upon VEGF-A stimulation (Figure 4A). Of note, maximal ATF-2–pT71 levels detected upon VEGF-A_{165} addition were approximately twofold to fivefold higher (Figure 4B) than comparable VEGF-A_{121} (Figure 4C) ligand concentrations.

Multiple signal transduction pathways, including JNK, p38 MAPK, ERK1/2, and ATM, stimulate phosphorylation at different sites on ATF-2 (Lau and Ronai, 2012). To assess whether the increase in phospho–ATF-2 was dependent on MEK1-ERK1/2 or p38 MAPK pathways, we used cell-permeable small-molecule inhibitors specific for either pathway (Figure 4D). VEGF-A–stimulated activation of ERK1/2 is significantly reduced by addition of U0126, a MEK1 inhibitor (Figure 4D). In contrast, VEGF-A–stimulated activation of p38 MAPK is significantly reduced by addition of SB203580, which inhibits both the α and β forms of p38 MAPK (Figure 4D). Quantification of VEGF-A–stimulated phospho–ATF-2 levels showed that that U0126 (MEK1 inhibitor) but not SB203580 (p38 MAPK inhibitor) completely blocked ligand-stimulated phosphorylation of ATF-2 (Figure 4E).

A key aspect of growth factor–stimulated MAPK activation is nuclear translocation of activated protein kinases and phosphorylation of key substrates, which in turn regulate gene transcription (Plotnikov *et al.*, 2011). We previously showed that VEGF-A stimulation causes translocation of activated ERK1/2 into the nucleus of endothelial cells (Jopling *et al.*, 2009). To correlate ERK1/2 translocation with ATF-2 activation, we monitored the intracellular distribution of phospho-ERK1/2 and ATF-2–pT71 using microscopy (Figure 4F). Activated phospho-ERK1/2 was detected in both the cytoplasm and nucleus within 15 min; this also correlated with a peak of phospho-ATF-2 in the nucleus (Figure 4F). Microscopy analysis of phospho-ERK1/2 and phospho-ATF-2 in the nucleus revealed substantial codistribution of both proteins at ~15 min post–VEGF-A_{165} stimulation (Figure 4G). Quantification of nuclear phospho-ERK1/2 and phospho–ATF-2 showed a >10-fold rise in codistribution after VEGF-A_{165} stimulation (Figure 4H). Such findings show a close link of VEGF-A_{165}–stimulated MAPK signal transduction leading to ERK1/2 activation, nuclear translocation, and downstream activation of ATF-2.

The VEGF-A coreceptor NRP1 has been shown to attenuate VEGF-A–stimulated signal transduction (Pan *et al.*, 2007; Herzog *et al.*, 2011). Therefore we evaluated whether NRP1 was essential for optimal VEGF-A–stimulated ATF-2 activation. Using immunoblotting, we monitored ATF-2–pT71 levels after 15 min of stimulation with either VEGF-A_{165} or VEGF-A_{121} in NRP1-depleted and control endothelial cells (Supplemental Figure S2A). Quantification revealed that both VEGF-A_{165}– and VEGF-A_{121}–stimulated ATF-2 activation was reduced in NRP1-depleted endothelial cells (Supplemental Figure S2B). One consequence of a reduction in NRP1 levels was a concomitant reduction in VEGF-A–stimulated ERK1/2 activation (Supplemental Figure S2C). These data suggest that NRP1 influences the ability of the VEGFR2–VEGF-A_{165} complex to effectively activate downstream ERK1/2 and thus ATF-2.

VEGF-A and ATF-2 are required for VCAM-1 expression and endothelial–leukocyte interactions

VEGF-A–stimulated VCAM-1 gene expression has implicated both the NF-κB pathway and forkhead transcription factors (Kim *et al.*, 2001a,b; Abid *et al.*, 2006; Dejana *et al.*, 2007). On the basis of our data, we hypothesized that ATF-2 acts as a nuclear "switch" for converting VEGF-A isoform–specific short-term cytosol-to-nucleus signaling (via the MEK1-ERK1/2 pathway) into VCAM-1 gene

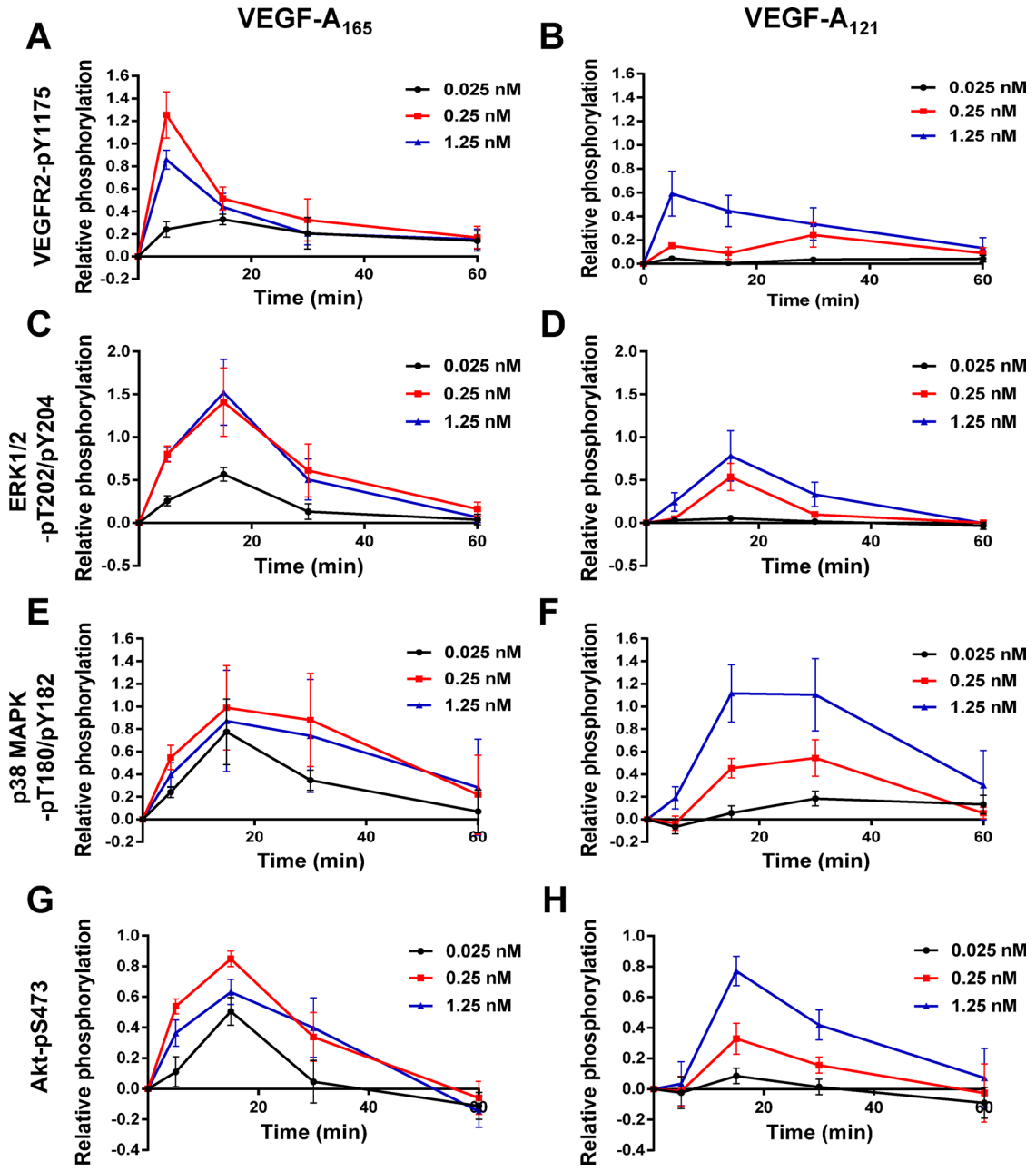

FIGURE 3: Quantification of VEGF-A isoform–specific signal transduction. Quantification of (A, B) VEGFR2-pY1175, (C, D) ERK1/2-pT202/pY204, (E, F) p38-pT180/pY182, and (G, H) Akt-pS473 levels upon (A, C, E, G) VEGF-A_{165} or (B, D, F, H) VEGF-A_{121} titration. Error bars indicate ±SEM ($n \geq 4$).

transcription, thus modulating VEGF-A isoform–specific long-term endothelial responses (including leukocyte recruitment). To evaluate ATF-2 requirement in VEGF-A–stimulated gene transcription, we first used specific small interfering RNA (siRNA) duplexes to deplete endothelial ATF-2. As expected, ATF-2 mRNA levels were depleted only in endothelial cells treated with ATF-2–specific siRNA duplexes (ATF-2 knockdown) in comparison to scrambled siRNA duplex treatment (control), under both nonstimulated and VEGF-A–stimulated conditions (Figure 5A). We then analyzed whether ATF-2 depletion affected VCAM-1 mRNA levels (Figure 5B). On VEGF-A_{165} stimulation, we detected ~1.4-fold increase in VCAM-1 mRNA levels compared with controls (Figure 5B). VEGF-A_{121}–stimulated endothelial cells produced ~1.2-fold increase in VCAM-1 mRNA levels, but this was substantially less than that observed for VEGF-A_{165} (Figure 5B). ATF-2 knockdown substantially reduced the VEGF-A–stimulated increase in VCAM-1 mRNA levels by ~25% (Figure 5B). There is thus a functional requirement for the presence of ATF-2 in VEGF-A–stimulated VCAM-1 expression in endothelial cells.

One question is the link between the requirement for ATF-2 in endothelial signal transduction and protein expression. To address this, we used immunoblotting to monitor protein levels and phosphorylation events 8 h after VEGF-A stimulation in control or ATF-2–depleted endothelial cells (Figure 5C). This time point of post–VEGF-A stimulation was used as the point of maximal ligand-stimulated VCAM-1 expression (Figure 1D). ATF-2 knockdown caused ~75% reduction in ATF-2 protein levels (Figure 5D). Activated VEGFR2-pY1175 levels were significantly elevated at this

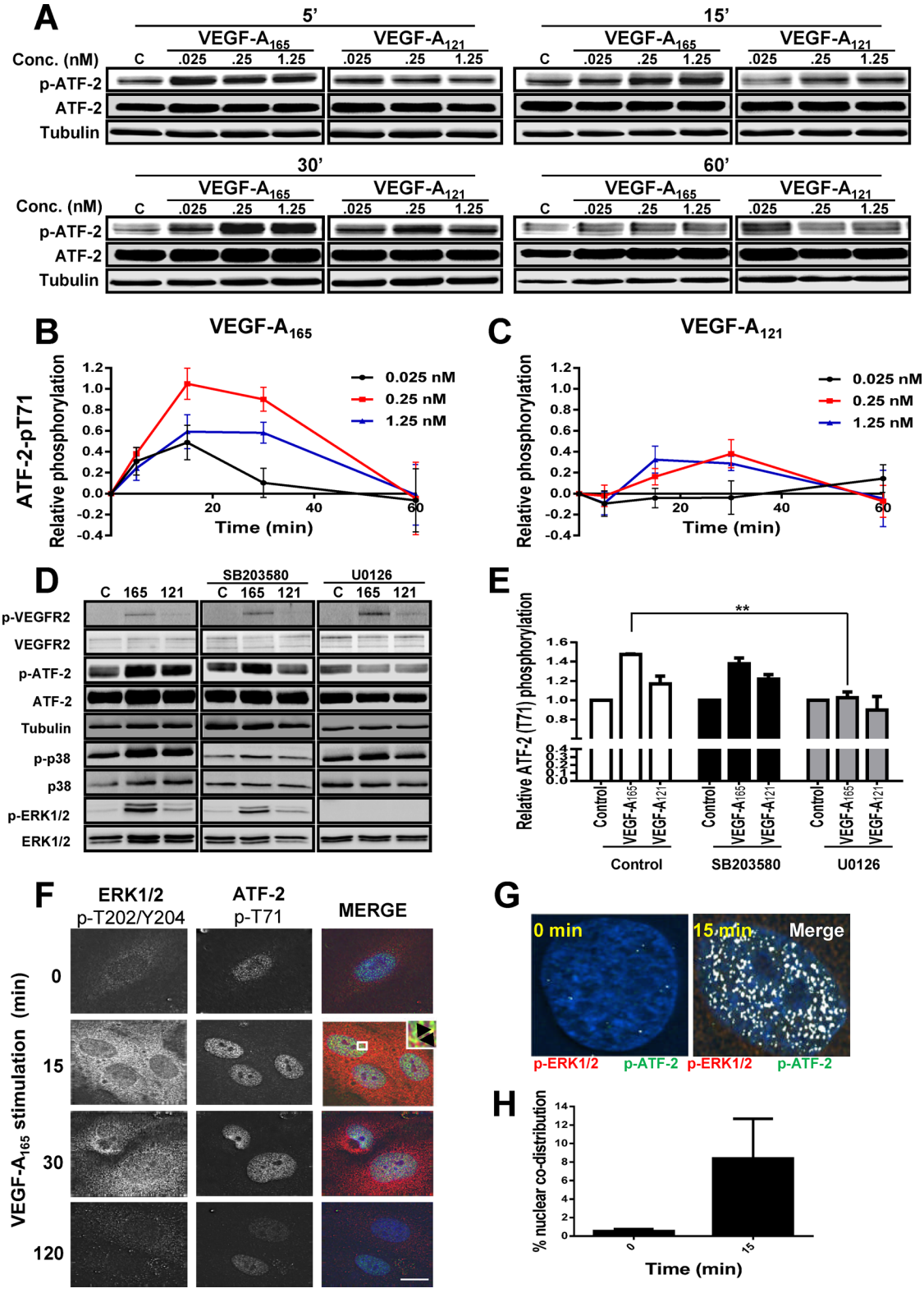

FIGURE 4: VEGF-A isoform–specific intracellular signaling regulates ATF-2 phosphorylation. (A) Immunoblotting of VEGF-A–stimulated endothelial cells for ATF-2-pT71, total ATF-2, and tubulin upon ligand titration. (B, C) Quantification of phosphorylated ATF-2-pT71 levels upon (B) VEGF-A_{165} and (C) VEGF-A_{121} titration. Error bars indicate ±SEM ($n = 4$). (D) Immunoblotting VEGFR2, ATF-2, ERK1/2, and p38 MAPK total and phosphorylated levels after preincubation with MEK1 inhibitor (U0126) or p38 MAPK inhibitor (SB203580), followed by VEGF-A isoform (1.25 nM) stimulation for 15 min. (E) Quantification of ATF-2-pT71 levels upon activation by VEGF-A_{165} or VEGF-A_{121} in the presence of MEK1 inhibitor (U0126) or p38 MAPK inhibitor (SB203580). Error bars indicate ±SEM ($n = 3$). (F) Endothelial cells stimulated with VEGF-A_{165} for 0, 15, or 30 min were processed for immunofluorescence microscopy using mouse

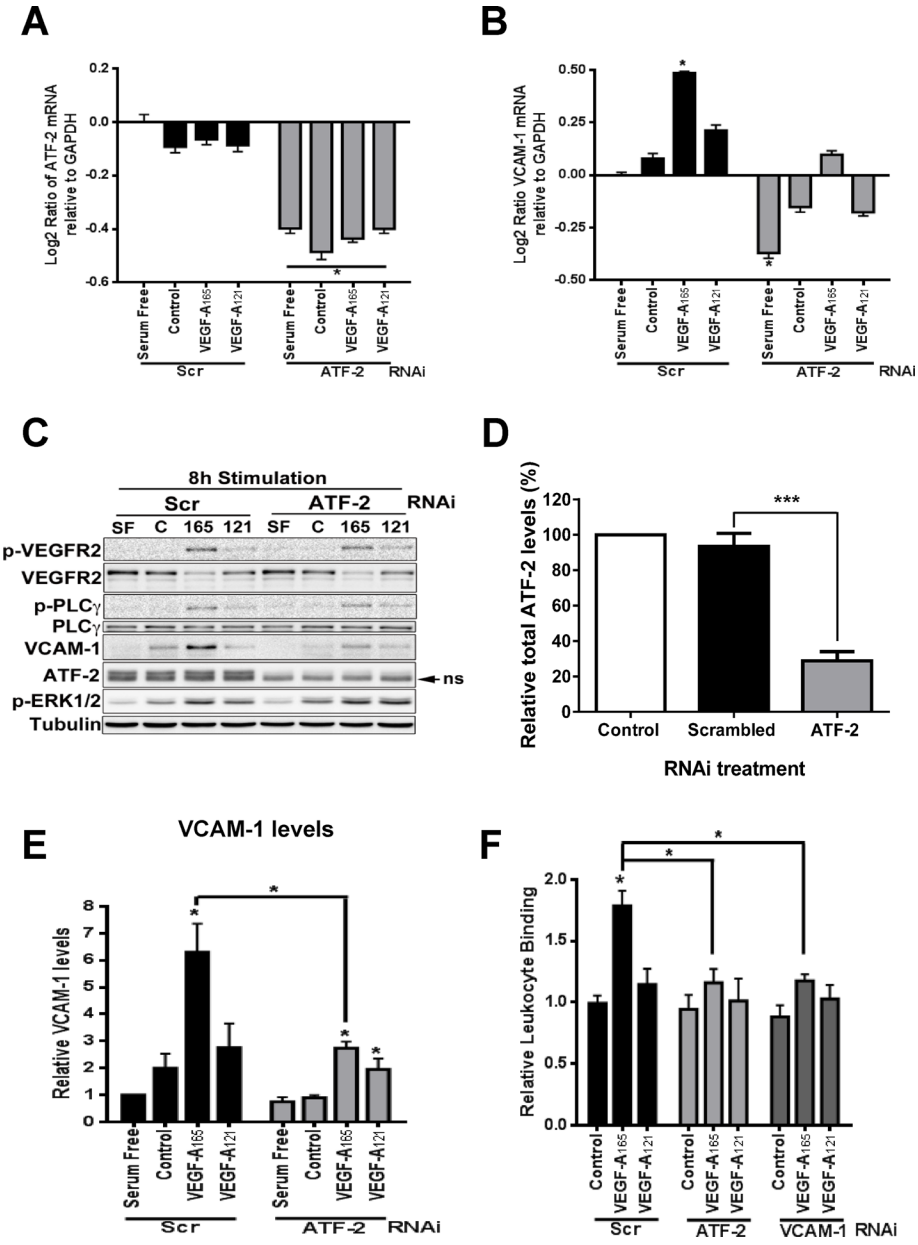

FIGURE 5: ATF-2 requirement for VEGF-A isoform–specific control of VCAM-1 expression in endothelial cells. (A, B) Endothelial cells stimulated with 0.25 nM VEGF-A_{165} or VEGF-A_{121} in different growth conditions for 4 h were analyzed by qRT-PCR for (A) ATF-2 or (B) VCAM-1 mRNA levels. GAPDH mRNA was used as an internal control. Error bars denote ±SEM ($n = 3$). (C) Endothelial cells subjected to RNA interference and knockdown with either scrambled (Scr) or ATF-2–specific (ATF-2) siRNA duplexes were then stimulated with 0.25 nM VEGF-A_{165} or VEGF-A_{121} for 8 h, lysed, and subjected to immunoblot analysis for a variety of proteins, including ATF-2, VEGFR2, and VCAM-1. (D) Quantification of ATF-2 knockdown in endothelial cells. Error bars indicate ±SEM ($n = 3$). (E) Quantification of VCAM-1 levels after 8 h of VEGF-A stimulation. Error bars denote ±SEM ($n \geq 3$). (F) Endothelial cells treated with scrambled (Scr), ATF-2, or VCAM-1 siRNA duplexes were stimulated with 0.25 nM VEGF-A_{165} or VEGF-A_{121} (7 h) before binding of calcein-labeled, activated HL-60 leukocytes and lysis and measurement (see *Materials and Methods*). Error bars denote ±SEM ($n \geq 3$). *$p < 0.05$, ***$p < 0.005$.

time point but were mirrored by a large decrease in VEGFR2 levels (Figure 5C). Differential phosphorylation in ERK1/2 and phospholipase Cγ1 was also evident (Figure 5C). These findings showed that ATF-2 knockdown did not significantly affect VEGFR2 turnover and downstream signal transduction in response to VEGF-A stimulation.

We probed for VCAM-1 expression in control or ATF-2–depleted cells 8 h after VEGF-A isoform stimulation (Figure 5C). VCAM-1 expression was clearly ATF-2 dependent (Figure 5C), and quantification highlighted a relatively large (greater than threefold) increase in VCAM-1 levels observed upon VEGF-A_{165} stimulation compared with cells incubated in serum-free or complete medium (Figure 5E). Depletion of ATF-2 reduced VCAM-1 to baseline levels in VEGF-A–stimulated cells (Figure 5E). VEGF-A_{121} also stimulated a smaller, 30–40% increase in VCAM-1 protein levels, which was also ATF-2 dependent (Figure 5, C and E). These data showed that increased VCAM-1 expression caused by VEGF-A not only was ATF-2 dependent but also influenced VCAM-1 mRNA levels.

Endothelial VCAM-1 binds leukocyte α4β1 integrin (VLA-4) and promotes leukocyte recruitment onto the endothelium before transendothelial migration (Sixt *et al.*, 2006; Nourshargh *et al.*, 2010; Reglero-Real *et al.*, 2012). A major question is whether VEGF-A–stimulated and ATF-2–dependent VCAM-1 expression can influence leukocyte binding to endothelial cells. To test this idea, we used a binding assay that monitored the binding of fluorescent-labeled human leukocyte HL-60 cells to an endothelial cell monolayer (Figure 5F). VEGF-A_{165} stimulated ~75% increase in leukocyte binding to the endothelial monolayer (Figure 5F). However, VEGF-A_{121} caused only a small, ~15% increase in leukocyte binding to endothelial cells (Figure 5F). ATF-2 knockdown completely ablated VEGF-A–stimulated binding of leukocytes to endothelial cells (Figure 5F). This phenomenon was VCAM-1 dependent, as VCAM-1 knockdown also completely inhibited endothelial–leukocyte interactions (Figure 5F). These data confirm that the VEGF-A–stimulated expression of endothelial VCAM-1 not only is ATF-2 dependent but also is sufficient to enable recruitment of leukocytes and enhance cell–cell interactions.

anti-ERK1/2-pT202/pY204 or rabbit anti-ATF-2-pT71, followed by fluorescence-labeled secondary antibodies. Overlay of phospho-ERK1/2 (red) and phospho-ATF-2 (green) staining patterns, with inset box indicating regions of codistribution within the nucleus (yellow). Bar, 10 μm. (G) Nuclear codistribution of phospho-ERK1/2 and phospho-ATF-2 (white) 15 min poststimulation. (H) Quantification of nuclear phospho-ERK1/2 and phospho-ATF-2 codistribution at 0 and 15 min after VEGF-A_{165} treatment. Error bars indicate ±SEM ($n = 3$). **$p < 0.01$.

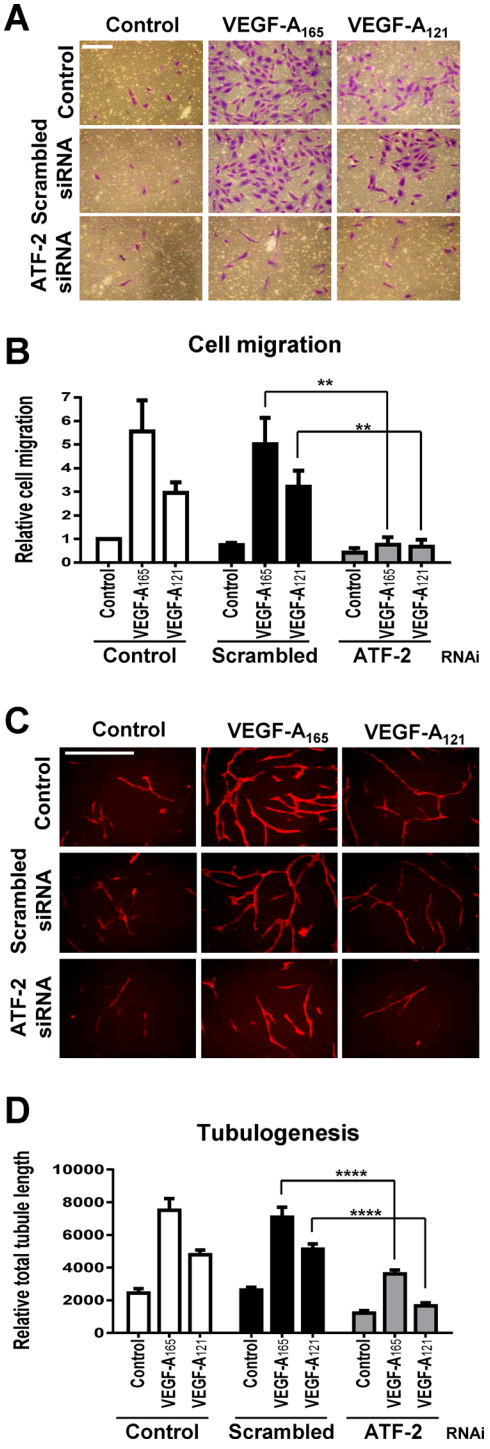

FIGURE 6: VEGF-A and ATF-2 regulation of endothelial cell responses. (A–D) Control, scrambled, or ATF-2–specific siRNA duplex–treated endothelial cells were seeded into different assays and stimulated with 0.25 nM VEGF-A_{165} or VEGF-A_{121} and assessed for endothelial cell (A, B) migration or (C, D) tubulogenesis. Bar, 200 μm (A, B), 400 μm (C, D). Error bars indicate ±SEM ($n = 3$). $^{**}p < 0.01$, $^{****}p < 0.001$.

ATF-2 is required for VEGF-A–stimulated endothelial cell responses

VEGF-A–stimulated signal transduction regulates diverse long-term responses in endothelial cells, such as cell migration and tubulogenesis (Chung and Ferrara, 2011; Koch *et al.*, 2011). This raises the question as to the importance of ATF-2 in endothelial cell function and responses such as cell migration and tubule formation (tubulogenesis). To address this, we first compared the roles of these two VEGF-A isoforms in promoting endothelial cell migration, tubulogenesis, and ex vivo angiogenesis. VEGF-A_{165} produced a marked dose-dependent stimulation in endothelial cell migration (Supplemental Figure S3, A and B) and tubulogenesis (Supplemental Figure S3, C and D). However, VEGF-A_{121} showed a much reduced or modest stimulation in such endothelial cell responses, and such effects were especially evident at intermediate or substoichiometric concentrations of VEGF-A (Supplemental Figure S3, B and D). Ex vivo angiogenesis assays using mouse aortic slices (Supplemental Figure S3E) showed VEGF-A_{165} had approximately threefold higher capacity to stimulate vascular sprouting (Supplemental Figure S3F). Thus each VEGF-A isoform had a distinct capacity to promote differential endothelial cell outputs; VEGF-A_{165} was generally more biologically active at low or substoichiometric concentrations.

This raised the question as to whether ATF-2 was equally important for such differential programming of these endothelial cell responses. ATF-2 knockdown completely abolished either VEGF-A_{165}– or VEGF-A_{121}–stimulated cell migration (Figure 6, A and B). ATF-2 knockdown also inhibited (~50%) both VEGF-A_{165}– and VEGF-A_{121}–stimulated tubulogenesis (Figure 6, C and D). ATF-2 was also required for endothelial cell proliferation (Supplemental Figure S4). Depletion of ATF-2 resulted in a approximately twofold decrease in VEGF-A_{165}–stimulated cell proliferation (Supplemental Figure S4). Of interest, depletion of ATF-2 also significantly reduced endothelial cell proliferation in complete media (Supplemental Figure S4).

Although VCAM-1 was required for endothelial–leukocyte adhesion (Figure 5F), this raised the possibility that it may also be required for other endothelial responses. To test this idea, we treated endothelial cells with scrambled or VCAM-1–specific siRNA duplexes before assessing VEGF-A isoform–specific endothelial tubulogenesis (Supplemental Figure S5, A and B). There was no significant difference in tubulogenesis between control and VCAM-1–depleted endothelial cells (Supplemental Figure S5B).

DISCUSSION

In this study, we show that different VEGF-A isoforms have differential capacities to regulate VCAM-1 gene expression and modulate endothelial–leukocyte binding via a novel mechanism (Figure 7). In this model, two VEGF-A isoforms with similar binding affinities differentially program VEGFR2 activation and downstream signal transduction to act on a common nuclear "switch" that regulates VCAM-1 expression. This "switch" comprised nuclear ATF-2, a transcription factor that is regulated by increased signal transduction from the MEK1-ERK1/2 pathway. Our findings show that ATF-2 is an important factor that regulates both VEGF-A–regulated responses and other essential pathways.

A key feature in VEGF-A–stimulated VCAM-1 expression is the requirement for ERK1/2 activation and ATF-2 expression. Maximal VCAM-1 expression is dependent on endothelial cell stimulation by a specific VEGF-A_{165} isoform. This isoform greatly increased VEGFR2 phosphorylation at residue Y1175 in comparison to the VEGF-A_{121} isoform. This correlated with an increased ability to promote ERK1/2 activation and nuclear translocation (Figure 7). Translocation of activated ERK1/2 into the nucleus revealed close proximity to activated phospho–ATF-2. It is feasible that the T71 residue on ATF-2 is directly phosphorylated by ERK1/2. Alternatively, another target of ERK1/2, such as the p90 ribosomal S6 kinase (p90rsk or MAPKAP-K1), can also translocate into the nucleus and phosphorylate key transcription factors (Arthur, 2008; Gerits *et al.*, 2008).

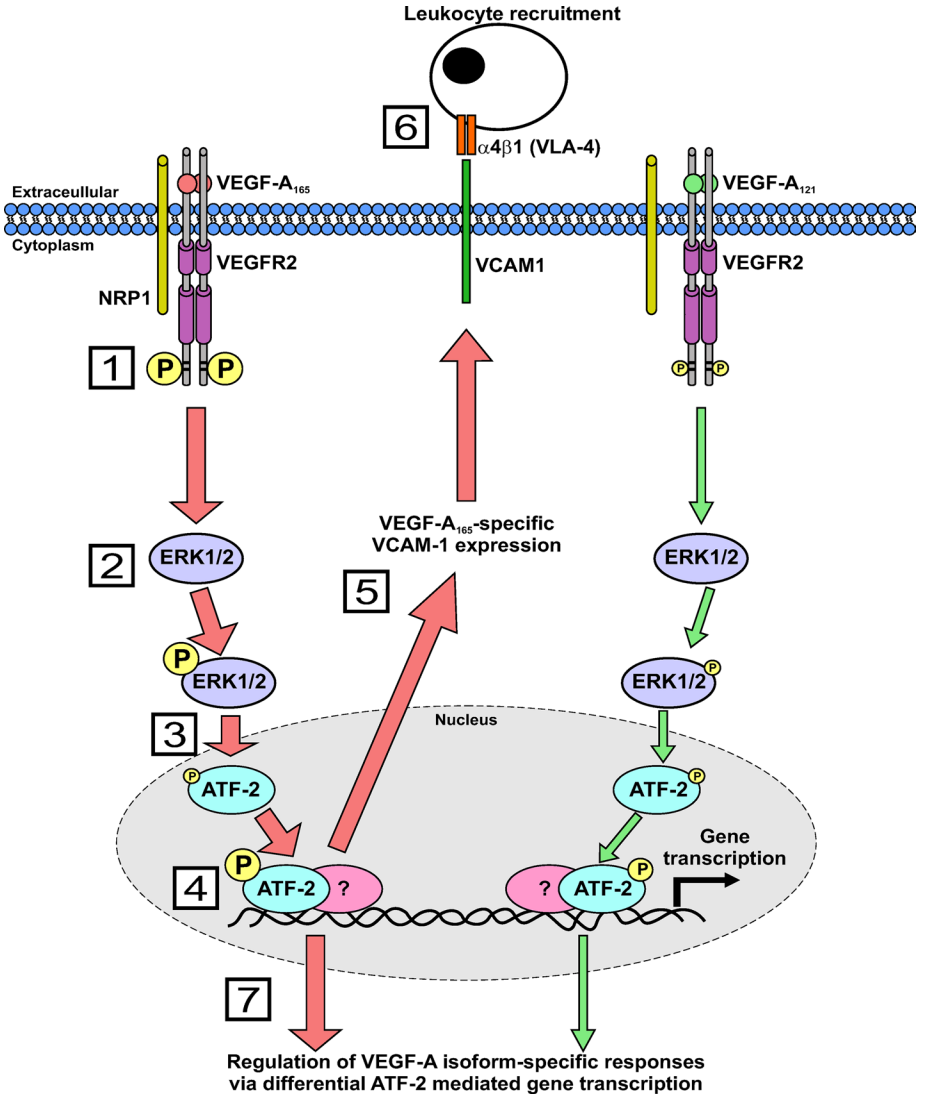

FIGURE 7: A mechanism for VEGF-A isoform–specific regulation of endothelial–leukocyte interactions. Schematic describing VEGF-A isoform–specific stimulation of intracellular signaling and ATF-2–regulated VCAM-1 gene expression. Numbered steps denote the following: 1) VEGFR2 activation by either VEGF-A_{165} or VEGF-A_{121} programs differential phosphorylation of residue Y1175; 2) VEGF-A_{165} stimulates elevated ERK1/2 phosphorylation and activation compared with VEGF-A_{121}; 3) phosphorylated ERK1/2 translocates to the nucleus and regulates ATF-2 phosphorylation; 4) VEGF-A_{165} is more potent than VEGF-A_{121} in promoting ATF-2 phosphorylation as a result of increased ERK1/2 activity; 5) VEGF-A_{165}–stimulated ATF-2 activity regulates VCAM-1 gene transcription; 6) VCAM-1 gene expression then promotes increased endothelial–leukocyte interactions; and 7) VEGF-A–stimulated ATF-2 activity also modulates other VEGF-A isoform–specific endothelial responses.

VEGF-A–stimulated intracellular signaling over a short time frame (0–2 h) caused early *VCAM-1* gene transcription and increased mRNA levels (2–8 h) with concomitant peak in VCAM-1 expression at the cell surface after 8 h. In this way, short-range signal transduction is translated into intermediate and long-range effects such as membrane protein expression and subsequent interactions that modulate endothelial interactions with the environment. A key feature is that two different VEGF-A isoforms of either 165 or 121 residues in length show significantly altered ability to promote VCAM-1 expression. This is largely due to decreased ERK1/2 activation by the shorter VEGF-A_{121} isoform. The different VEGF-A isoforms have a conserved N-proximal region (residues 1–111) and variable C-terminus (112–206). Of note, all VEGF-A isoforms display similar binding affinity to VEGFR2 (Keyt *et al.*, 1996; Delcombel *et al.*, 2013), but unique receptor–ligand complexes can produce different functional outputs. Of interest, it has been noted that the murine orthologues of VEGF-A_{121} and VEGF-A_{165} show capacity to differentially elevate expression of another cell adhesion molecule, ICAM-1, in the mouse ocular endothelium (Usui *et al.*, 2004). The underlying mechanism regulating such differential VEGF-A–regulated ICAM-1 expression is unknown but raises the speculation that ATF-2 may be involved in this phenomenon as well. In this context, it is well known that different VEGF-A isoforms have the capacity to trigger differential VEGFR2 activation and downstream signal transduction (Zhang *et al.*, 2000, 2008; Bates *et al.*, 2002; Nakatsu *et al.*, 2003; Herve *et al.*, 2005; Chen *et al.*, 2010). An important question concerns the mechanism underlying VEGF-A–stimulated gene transcription (Goddard and Iruela-Arispe, 2013). STAT3 (Bartoli *et al.*, 2003), Egr3 (Liu *et al.*, 2003), forkhead-like transcription factors (Abid *et al.*, 2006), FoxO- and Ets-related factors (Dejana *et al.*, 2007), and HLX (Testori *et al.*, 2011) have all been implicated in regulating VEGF-A–dependent gene transcription.

How ATF-2 regulates VCAM-1 gene transcription is intriguing. ATF-2 was originally identified as a nuclear transcriptional switch that was activated upon DNA damage or stress, thus enabling gene expression linked to an antiapoptotic response or cell proliferation (Lau and Ronai, 2012). The ATF-2 polypeptide can undergo phosphorylation at different Ser/Thr residues at the N-terminus (T52, S62, T69, T71, S73, S121) or C-terminus (S490, S498; Lau and Ronai, 2012). One possibility is that phospho–ATF-2 directly binds to the VCAM-1 promoter to stimulate early gene transcription: this may occur via the formation of ATF-2 homodimers or heterodimers with factors such as c-jun. In addition, ATF-2 may recruit other factors such as p300 (Kawasaki *et al.*, 1998) or IRF3 (Panne *et al.*, 2004) to promoter loci, which further modulate target gene expression. It has also been proposed that ATF-2 has intrinsic histone acetyltransferase activity (HAT) such that it acts to derepress gene transcription upon recruitment (Kawasaki *et al.*, 2000), and other transcription factors such as NF-κB or forkhead could directly stimulate *VCAM-1* gene transcription.

Our study shows evidence that different VEGF-A isoforms regulate both angiogenesis and inflammation via an ATF-2–dependent mechanism. The increased recruitment of activated leukocytes to VEGF-A_{165}–stimulated cells, in contrast to VEGF-A_{121}-stimulation, argues that this has a functional role in vivo. This could be useful in the VEGF-A isoform–specific recruitment of leukocytes into a developing blood vessel during angiogenesis. This would be useful in controlling vascular development and endothelial–leukocyte

balance within a vascular niche. Alternatively, such a phenomenon could be extremely useful during pathogenic infection or injury: the release of specific VEGF-A isoforms into the damaged vasculature not only could promote leukocyte recruitment but also could attune leukocyte recruitment to the extent of infection or injury. VEGF-A_{165} has been shown to stimulate VCAM-1 expression (Kim *et al.*, 2001a; Abid *et al.*, 2006), but this has also been contradicted (Stannard *et al.*, 2007). In this context, it has been shown that proinflammatory cytokines such as interleukin 1β or tumor necrosis factor α (TNFα) promote NF-κB, SP1, AP-1, and IRF recruitment to the *VCAM-1* locus to stimulate VCAM-1 expression (Collins *et al.*, 1995; Weber, 1996; Hordijk, 2006; Sixt *et al.*, 2006). A link between ATF-2 and NF-κB has also been proposed in regulating VCAM-1 expression during shear stress (Cuhlmann *et al.*, 2011). Expression of a mutant ATF-2 in a mouse model has been shown to inhibit VCAM-1 expression (Reimold *et al.*, 2001).

The interactions between endothelial cells and leukocytes can be subverted in major disease states ranging from atherosclerosis, rheumatoid arthritis, and pathogenic infection to cancer. This study now provides a mechanism to explain how different VEGF-A isoforms regulate not only angiogenesis but also inflammation in such disease states. Immune cells are well known to secrete proangiogenic cytokines such as TNFα and vascular endothelial growth factor A (VEGF-A; Griffioen and Molema, 2000; Naldini and Carraro, 2005). The angiocrine model postulated by Rafii and colleagues suggests that the endothelium secretes soluble and membrane-bound factors that act in a paracrine manner on neighboring cells to influence vascular development in tissues such as liver (Butler *et al.*, 2010; Ding *et al.*, 2010). Our work shows that VEGF-A isoforms have unique abilities to instruct the endothelium and influence leukocyte recruitment at local sites through cell–cell interactions. It will be a challenge to decipher the myriad of biological properties of the VEGF family with functional roles in both angiogenesis and inflammation in healthy and diseased states.

MATERIALS AND METHODS

Antibodies and growth factors

Antibodies were goat anti-VEGFR2 (R&D Systems, Minneapolis, MN), rabbit anti-ERK1/2, mouse anti–phospho-ERK1/2 (Thr^{202}/Tyr^{204}), rabbit anti-p38, rabbit anti–phospho-p38 (Thr^{180}/Tyr^{182}), rabbit anti–phospho-VEGFR2 (Tyr^{1175}), rabbit anti–ATF-2, rabbit anti–phospho-ATF-2 (Thr^{71}), rabbit anti-NRP1 (Cell Signaling Technology, Danvers, MA), mouse anti–α-tubulin, mouse anti–PECAM-1 (CD31; Santa Cruz Biotechnology, Santa Cruz, CA), and mouse anti–VCAM-1 (DAKO, Glostrup, Denmark).

Reagents were as follows. Endothelial cell growth medium (ECGM) was from PromoCell (Heidelberg, Germany). Scrambled, ATF-2, NRP1, and VCAM1 siRNA duplexes were purchased as siGENOME SMARTpools from Dharmacon (Thermo Scientific, Lafayette, CO) unless otherwise stated in the figure legends. Recombinant human VEGF-A_{165} was from Genentech (San Francisco, CA), and VEGF-A_{121} was from Promocell.

Cell culture, immunoblotting, and immunofluorescence studies

Human umbilical vein endothelial cells (HUVECs) were prepared as previously described (Howell *et al.*, 2004). Cells were seeded into six-well plates and cultured (for at least 24 h) in ECGM until ~80% confluent, washed three times with phosphate-buffered saline (PBS), and then starved in MCDB131 plus 0.2% (wt/vol) bovine serum albumin (BSA) for 2–3 h. HUVECs were then stimulated with 0, 0.025, 0.25, or 1.25 nM VEGF-A isoform for the desired time period. Cells were then washed three times with ice-cold PBS and lysed in buffer with 2% (wt/vol) SDS, Tris-buffered saline, 1 mM phenylmethylsulfonyl fluoride, and protease inhibitor cocktail (Sigma-Aldrich, Poole, United Kingdom). Protein concentration was determined using the bicinchoninic acid assay (ThermoFisher, Loughborough, United Kingdom). A 25 μg amount of protein lysate was subjected to SDS–PAGE before analysis by immunoblotting. For immunofluorescence analysis, cells were serum starved for 3 h before being stimulated with VEGF-A_{165}. Cells were fixed and processed as previously described (Bruns *et al.*, 2010). Images were acquired using a DeltaVision wide-field deconvolution microscope (Applied Precision, Issaquah, WA). Relative colocalization was quantified using ImageJ (National Institutes of Health, Bethesda, MD) as previously described (Bruns *et al.*, 2010; Jopling *et al.*, 2011).

Pharmacological inhibition of signal transduction

Cells were seeded and starved as stated previously, then pretreated with 10 μM SB203580 or U0126 (LC Labs, Boston, MA) for 30 min before stimulation with 1.25 nM VEGF-A isoform in MCDB131 plus 0.2% (wt/vol) BSA for 15 min. Cells were then processed via SDS–PAGE before immunoblot analysis.

Lipid-based transfection of siRNA duplexes

Cells were reversed transfected with siRNA duplexes using Lipofectamine RNAiMAX (Invitrogen, Paisley, United Kingdom). Per well of a six-well plate, 15 μl of 2 μM siRNA duplexes was added to 481 μl of serum/antibiotic-free OptiMEM (Invitrogen) and allowed to settle at room temperature for 5 min. Then 4 μl of Lipofectamine was added, and the mixture was inverted briefly and incubated at room temperature for 20 min. HUVECs were seeded at 2.5×10^5 cells/ml in a 1 ml volume of OptiMEM, followed by immediate dropwise addition of the siRNA/Lipofectamine mixture. Cells were left at room temperature for 30 min before being returned to the incubator. After 6 h total of incubation, medium was replaced for ECGM. Cells were allowed to recover for 72 h before treatment or processing for analysis.

Quantitative reverse transcription PCR

HUVECs were treated with siRNA duplexes specific for either ATF-2 or a scrambled (Scr) sequence for 72 h before growth arrest induced by overnight serum starvation (serum free) and 2 mM thymidine supplementation. Control cells were released for 4 h in full growth medium together with either 0.25 nM VEGF-A_{165} or VEGF-A_{121} before extraction of total RNA with the RNeasy Plus Mini Kit (Qiagen, Manchester, United Kingdom). A 1 μg total amount of RNA was reverse transcribed using the GoScript Reverse Transcription System (Promega, Southampton, United Kingdom). Real-time quantitative reverse transcription PCR (qRT-PCR) was performed using Power SYBR Green master mix (Applied Biosystems, Warrington, United Kingdom) with the following primer sets: glyceraldehyde-3-phosphate dehydrogenase (GAPDH; endogenous control), forward primer 5′-GTC TCC TCT GAC TTC AAC AGC G-3′, reverse primer 5′-ACC ACC CTG TTG CTG TAG CCA A-3′; ATF-2, forward primer 5′-GGT AGC GGA TTG GTT AGG ACT C-3′, reverse primer 5′TGC TCT TCT CCG ACG ACC ACT T-3′; and VCAM-1, forward primer 5′-GAT TCT GTG CCC ACA GTA AGG C-3′, reverse primer 5′TGG TCA CAG AGC CAC CTT CTT G-3′. qRT-PCR was carried out in multiwell plates run on an ABI 7900HT Fast Real-Time PCR System (Applied Biosystems) and gene expression analyzed using the ΔΔ*CT* method standardized against an endogenous control, GAPDH.

Leukocyte-binding assay

We labeled 2×10^5 HL-60 leukocytes/well with 0.5 µg/ml calcein (Invitrogen) for 30 min at 37°C. Cells were then pelleted and washed twice in 5 ml RPMI plus 10% (vol/vol) fetal calf serum (Invitrogen). Cells were left for 30 min at 37°C to allow deesterification of calcein agent. Then 100 nM phorbol 12-myristate 13-acetate (PMA; Sigma-Aldrich, Poole, United Kingdom) was added to the cells and left to incubate for 30 min at 37°C. Cells were again pelleted and washed twice in 5 ml RPMI. Then 2×10^5 HL-60 leukocytes/well were added onto a confluent layer of HUVECs that had been previously stimulated with full growth medium (±VEGF-A_{165} or VEGF-A_{121} for 7 h) and left to adhere for 1 h at 37°C. Nonadhered leukocytes were removed by gentle rinsing with PBS. Cells were then lysed in 200 µl of RIPA buffer. Then 50 µl was analyzed by fluorescence excitation at 488 nm and emission at 520 nm in a multiwall plate format using a 96-well FLUOstar OPTIMA florescence plate reader (BMG LABTECH, Aylesbury, United Kingdom). Values were compared with controls where VEGF-A was absent.

Cell migration assay

HUVECs were seeded at 3×10^4 cells/well into a 8 µm pore size Transwell filter inserted into a 24-well companion plate (BD Biosciences, Oxford, United Kingdom) in MCDB131 plus 0.2% (wt/vol) BSA. ECGM or MCDB131 plus 0.2% (wt/vol) BSA containing the desired concentration of VEGF-A was added to the lower chambers to stimulate cell migration. Cells were allowed to migrate for 24 h before being fixed and stained with 0.2% (wt/vol) crystal violet in 20% (vol/vol) methanol. Nonmigrated cells were then removed from the upper chamber using a moist cotton bud. Three to five random fields were imaged per Transwell filter and the average number of migratory cells calculated.

Tubulogenesis assay

Primary human foreskin fibroblasts (Promocell) were cultured to confluency in 48-well plates in Q333 fibroblast growth medium (PAA Laboratories, Pasching, Austria). Then 6500 HUVECs were seeded onto the fibroblast monolayer in a 1:1 mixture of Q333 and ECGM and left for 24 h. Medium was then removed and replaced with fresh ECGM ± VEGF-A as desired; medium was replaced every 2–3 d for 7 d. Cocultures were then fixed in 200 µl for 20 min and blocked in 1% (wt/vol) BSA for 30 min at room temperature. Cocultures were then incubated with 1 µg/ml mouse anti-human PECAM-1 (CD31; Santa Cruz Biotechnology, Santa Cruz, CA) overnight at room temperature. Cells were washed three times with PBS before incubation with donkey secondary antibody anti-mouse Alexa Fluor 594 conjugate (Invitrogen) for 2–3 h at room temperature. Wells were then washed three times with PBS. Endothelial tubules were then visualized by immunofluorescence microscopy using an EVOS-fl inverted digital microscope (Life Technologies). Five random fields were imaged per well. Both the number of branch points and the total tubule length were then quantified from each photographic field using the open source software AngioQuant (www.cs.tut.fi/sgn/csb/angioquant) and values averaged. For a more detailed method see Fearnley *et al.* (2014).

Ex vivo aortic sprouting assay

This protocol was adapted from previous studies (Baker *et al.*, 2012). All animal and tissue procedures were carried out in accordance with United Kingdom Home Office regulations and guidance at room temperature unless otherwise stated. Briefly, male wild-type C57Bl/6 mice were killed in accordance with United Kingdom Home Office regulations. Thoracic aorta was harvested from aortic arch to diaphragm and flushed with 500 µl of Hank's balanced salt solution to remove blood products. Fat and fascia were cleaned from the aorta by sharp dissection and the vessel sliced into 0.5-mm rings with a scalpel. Rings were serum starved overnight at 37°C in 5 ml OptiMEM supplemented with penicillin-streptomycin. On ice, purified type 1 rat-tail collagen (Millipore, Watford, United Kingdom) was diluted to 1 mg/ml with DMEM before adding 2 µl/ml of 5 M NaOH. A 55 µl amount of this embedding matrix was pipetted per well into a 96-well plate and aortic ring submerged within. Plates were left for 15 min at room temperature before incubation at 60 min at 37°C. A 150 µl amount of OptiMEM containing 2.5% (vol/vol) FCS and penicillin-streptomycin was added per well with appropriate VEGF-A. Aortic rings were incubated at 37°C for 5 d with a medium change on day 3. Wells were washed with 150 µl of PBS containing 2 mM $CaCl_2$ and 2 mM $MgCl_2$ and fixed in 4% (vol/vol) Formalin for 30 min. The collagen was permeabilized with three 15 min washes with PBS buffer containing 2 mM $MgCl_2$, 2 mM $CaCl_2$, and 0.25% (vol/vol) Triton X-100. Rings were blocked in 30 µl of 1% (wt/vol) BSA in PBLEC (PBS containing 100 µM $MnCl_2$, 1% [vol/vol] Tween-20, 2 mM $CaCl_2$, 2 mM $MgCl_2$) for 30 min at 37°C. A 2.5 µg amount of BS1 lectin–fluorescein isothiocyanate (Sigma-Aldrich) in PBLEC was added per well, followed by overnight incubation at 4°C. Wells were washed three times with 100 µl of PBS containing 2 mM $MgCl_2$, 2 mM $CaCl_2$, and 0.25% (vol/vol) Triton X-100 and incubated for 2 h with 1 µg/ml 4′,6-diamidino-2-phenylindole (in PBLEC). Wells were washed three times with 100 µl PBS containing 0.1% (vol/vol) Triton X-100 and then with 100 µl of sterile water. Aortic sprouts were imaged using an EVOS-fl inverted digital microscope (Life Technologies). The number of initial sprouts (vascular sprouts emanating directly from the aortic ring) was counted, and sprout intensity (total image intensity – aortic ring intensity) was determined using ImageJ software.

Endothelial cell proliferation assay

Two thousand endothelial cells were seeded per well of a 96-well plate and left to acclimatize in complete growth medium overnight. On the next day, medium was changed and cells starved in MCDB131 medium plus 0.2% BSA (wt/vol) for 3 h. Cells were then stimulated with the desired concentration of VEGF-A isoforms in a final 100 µl volume for 24 h. Bromodeoxyuridine, 10 µM, was added per well after 20 h. A cell proliferation enzyme-linked immunosorbent assay was then used according to manufacturer's instructions (Roche Diagnostics, Mannheim, Germany). The color change was developed using 3,3′,5,5′-tetramethylbenzidine solution and the reaction quenched with 1 M H_2SO_4. Absorbance was measured at 450 nm using a variable-wavelength 96-well plate reader (Tecan, Mannedorf, Switzerland).

Statistical analysis

This was performed using a one-way analysis of variance (ANOVA), followed by Tukey's post hoc test or two-way ANOVA followed by Bonferroni multiple comparison test, using Prism software (GraphPad, La Jolla, CA). Significant differences between control and test groups were evaluated with $*p < 0.05$, $**p < 0.01$, $***p < 0.005$, and $****p < 0.001$ indicated on the graphs. Error bars in graphs and histograms denote ±SEM.

ACKNOWLEDGMENTS

We thank David Beech for comments on the manuscript and Annette Weninger for technical help. This work was supported by a Heart Research UK PhD studentship (G.W.F.), a Circulation Foundation George Davies Surgeon Scientist Award (N.A.M.),

British Heart Foundation and Medical Research Council project grants (S.B.W.), a British Heart Foundation program grant (I.C.Z.), and a Medical Research Council project grant (A.F.B.). S.B.W. is the holder of a European Research Council Fellowship.

REFERENCES

Abid MR, Nadeau RJ, Spokes KC, Minami T, Li D, Shih SC, Aird WC (2008). Hepatocyte growth factor inhibits VEGF-forkhead-dependent gene expression in endothelial cells. Arterioscler Thromb Vasc Biol 28, 2042–2048.

Abid MR, Shih SC, Otu HH, Spokes KC, Okada Y, Curiel DT, Minami T, Aird WC (2006). A novel class of vascular endothelial growth factor-responsive genes that require forkhead activity for expression. J Biol Chem 281, 35544–35553.

Arthur JS (2008). MSK activation and physiological roles. Front Biosci 13, 5866–5879.

Baker M, Robinson SD, Lechertier T, Barber PR, Tavora B, D'Amico G, Jones DT, Vojnovic B, Hodivala-Dilke K (2012). Use of the mouse aortic ring assay to study angiogenesis. Nature Prot 7, 89–104.

Bartoli M, Platt D, Lemtalsi T, Gu X, Brooks SE, Marrero MB, Caldwell RB (2003). VEGF differentially activates STAT3 in microvascular endothelial cells. FASEB J 17, 1562–1564.

Bates DO, Cui TG, Doughty JM, Winkler M, Sugiono M, Shields JD, Peat D, Gillatt D, Harper SJ (2002). VEGF165b, an inhibitory splice variant of vascular endothelial growth factor, is down-regulated in renal cell carcinoma. Cancer Res 62, 4123–4131.

Bruns AF, Bao L, Walker JH, Ponnambalam S (2009). VEGF-A-stimulated signalling in endothelial cells via a dual receptor tyrosine kinase system is dependent on co-ordinated trafficking and proteolysis. Biochem Soc Trans 37, 1193–1197.

Bruns AF, Herbert SP, Odell AF, Jopling HM, Hooper NM, Zachary IC, Walker JH, Ponnambalam S (2010). Ligand-stimulated VEGFR2 signaling is regulated by co-ordinated trafficking and proteolysis. Traffic 11, 161–174.

Butler JM, Kobayashi H, Rafii S (2010). Instructive role of the vascular niche in promoting tumour growth and tissue repair by angiocrine factors. Nat Rev Cancer 10, 138–146.

Carmeliet P *et al.* (1996). Abnormal blood vessel development and lethality in embryos lacking a single VEGF allele. Nature 380, 435–439.

Chen TT, Luque A, Lee S, Anderson SM, Segura T, Iruela-Arispe ML (2010). Anchorage of VEGF to the extracellular matrix conveys differential signaling responses to endothelial cells. J Cell Biol 188, 595–609.

Chung AS, Ferrara N (2011). Developmental and pathological angiogenesis. Annu Rev Cell Dev Biol 27, 563–584.

Collins T, Read MA, Neish AS, Whitley MZ, Thanos D, Maniatis T (1995). Transcriptional regulation of endothelial cell adhesion molecules: NF-kappa B and cytokine-inducible enhancers. FASEB J 9, 899–909.

Cuhlmann S *et al.* (2011). Disturbed blood flow induces RelA expression via c-Jun N-terminal kinase 1: a novel mode of NF-KB regulation that promotes arterial inflammation. Circ Res 108, 950–959.

Dejana E, Taddei A, Randi AM (2007). Foxs and Ets in the transcriptional regulation of endothelial cell differentiation and angiogenesis. Biochim Biophys Acta 1775, 298–312.

Delcombel R *et al.* (2013). New prospects in the roles of the C-terminal domains of VEGF-A and their cooperation for ligand binding, cellular signaling and vessels formation. Angiogenesis 16, 353–371.

Ding BS *et al.* (2010). Inductive angiocrine signals from sinusoidal endothelium are required for liver regeneration. Nature 468, 310–315.

Ewan LC, Jopling HM, Jia H, Mittar S, Bagherzadeh A, Howell GJ, Walker JH, Zachary IC, Ponnambalam S (2006). Intrinsic tyrosine kinase activity is required for vascular endothelial growth factor receptor 2 ubiquitination, sorting and degradation in endothelial cells. Traffic 7, 1270–1282.

Fearnley GW, Smith GA, Odell AF, Latham AM, Wheatcroft SB, Harrison MA, Tomlinson DC, Ponnambalam S (2014). Vascular endothelial growth factor a-stimulated signaling from endosomes in primary endothelial cells. Methods Enzymol 535, 265–292.

Gerits N, Kostenko S, Shiryaev A, Johannessen M, Moens U (2008). Relations between the mitogen-activated protein kinase and the cAMP-dependent protein kinase pathways: comradeship and hostility. Cell Signal 20, 1592–1607.

Goddard LM, Iruela-Arispe ML (2013). Cellular and molecular regulation of vascular permeability. Thromb Haemost 109, 407–415.

Griffioen AW, Molema G (2000). Angiogenesis: potentials for pharmacologic intervention in the treatment of cancer, cardiovascular diseases, and chronic inflammation. Pharm Rev 52, 237–268.

Harper SJ, Bates DO (2008). VEGF-A splicing: the key to anti-angiogenic therapeutics? Nat Rev Cancer 8, 880–887.

Herve MA, Buteau-Lozano H, Mourah S, Calvo F, Perrot-Applanat M (2005). VEGF189 stimulates endothelial cells proliferation and migration in vitro and up-regulates the expression of Flk-1/KDR mRNA. Exp Cell Res 309, 24–31.

Herzog B, Pellet-Many C, Britton G, Hartzoulakis B, Zachary IC (2011). VEGF binding to NRP1 is essential for VEGF stimulation of endothelial cell migration, complex formation between NRP1 and VEGFR2, and signaling via FAK Tyr407 phosphorylation. Mol Biol Cell 22, 2766–2776.

Holmqvist K, Cross MJ, Rolny C, Hagerkvist R, Rahimi N, Matsumoto T, Claesson-Welsh L, Welsh M (2004). The adaptor protein shb binds to tyrosine 1175 in vascular endothelial growth factor (VEGF) receptor-2 and regulates VEGF-dependent cellular migration. J Biol Chem 279, 22267–22275.

Hordijk PL (2006). Endothelial signalling events during leukocyte transmigration. FEBS J 273, 4408–4415.

Horowitz A, Seerapu HR (2012). Regulation of VEGF signaling by membrane traffic. Cell Signal 24, 1810–1820.

Howell GJ *et al.* (2004). Endothelial cell confluence regulates Weibel-Palade body formation. Mol Membr Biol 21, 413–421.

Jain RK, Koenig GC, Dellian M, Fukumura D, Munn LL, Melder RJ (1996). Leukocyte-endothelial adhesion and angiogenesis in tumors. Cancer Metastasis Rev 15, 195–204.

Jopling HM, Howell GJ, Gamper N, Ponnambalam S (2011). The VEGFR2 receptor tyrosine kinase undergoes constitutive endosome-to-plasma membrane recycling. Biochem Biophys Res Commun 410, 170–176.

Jopling HM, Odell A, Hooper NM, Zachary IC, Walker JH, Ponnambalam S (2009). Rab GTPase Regulation of VEGFR2 trafficking and signaling in endothelial cells. Arterioscler Thromb Vasc Biol 29, 1119–1124.

Karihaloo A, Karumanchi SA, Cantley WL, Venkatesha S, Cantley LG, Kale S (2005). Vascular endothelial growth factor induces branching morphogenesis/tubulogenesis in renal epithelial cells in a neuropilin-dependent fashion. Mol Cell Biol 25, 7441–7448.

Kawasaki H, Schiltz L, Chiu R, Itakura K, Taira K, Nakatani Y, Yokoyama KK (2000). ATF-2 has intrinsic histone acetyltransferase activity which is modulated by phosphorylation. Nature 405, 195–200.

Kawasaki H, Song J, Eckner R, Ugai H, Chiu R, Taira K, Shi Y, Jones N, Yokoyama KK (1998). p300 and ATF-2 are components of the DRF complex, which regulates retinoic acid- and E1A-mediated transcription of the c-jun gene in F9 cells. Genes Dev 12, 233–245.

Keyt BA, Berleau LT, Nguyen HV, Chen H, Heinsohn H, Vandlen R, Ferrara N (1996). The carboxyl-terminal domain (111–165) of vascular endothelial growth factor is critical for its mitogenic potency. J Biol Chem 271, 7788–7795.

Kim I, Moon SO, Kim SH, Kim HJ, Koh YS, Koh GY (2001a). Vascular endothelial growth factor expression of intercellular adhesion molecule 1 (ICAM-1), vascular cell adhesion molecule 1 (VCAM-1), and E-selectin through nuclear factor-kappa B activation in endothelial cells. J Biol Chem 276, 7614–7620.

Kim I, Moon SO, Park SK, Chae SW, Koh GY (2001b). Angiopoietin-1 reduces VEGF-stimulated leukocyte adhesion to endothelial cells by reducing ICAM-1, VCAM-1, and E-selectin expression. Circ Res 89, 477–479.

Koch S, Claesson-Welsh L (2012). Signal transduction by vascular endothelial growth factor receptors. Cold Spring Harb Perspect Med 2, a006502.

Koch S, Tugues S, Li X, Gualandi L, Claesson-Welsh L (2011). Signal transduction by vascular endothelial growth factor receptors. Biochem J 437, 169–183.

Lau E, Ronai ZA (2012). ATF2—at the crossroad of nuclear and cytosolic functions. J Cell Sci 125, 2815–2824.

Lemmon MA, Schlessinger J (2010). Cell signaling by receptor tyrosine kinases. Cell 141, 1117–1134.

Liu D, Jia H, Holmes DI, Stannard A, Zachary I (2003). Vascular endothelial growth factor-regulated gene expression in endothelial cells: KDR-mediated induction of Egr3 and the related nuclear receptors Nur77, Nurr1, and Nor1. Arterioscler Thromb Vasc Biol 23, 2002–2007.

Meadows KL, Hurwitz HI (2012). Anti-VEGF therapies in the clinic. Cold Spring Harb Perspect Med 2, a006577.

Melder RJ, Koenig GC, Witwer BP, Safabakhsh N, Munn LL, Jain RK (1996). During angiogenesis, vascular endothelial growth factor and basic fibroblast growth factor regulate natural killer cell adhesion to tumor endothelium. Nat Med 2, 992–997.

Nakatsu MN, Sainson RC, Perez-del-Pulgar S, Aoto JN, Aitkenhead M, Taylor KL, Carpenter PM, Hughes CC (2003). VEGF(121) and VEGF(165) regulate blood vessel diameter through vascular endothelial growth

factor receptor 2 in an in vitro angiogenesis model. Lab Invest 83, 1873–1885.
Nakayama M, Berger P (2013). Coordination of VEGF receptor trafficking and signaling by coreceptors. Exp Cell Res 319, 1340–1347.
Naldini A, Carraro F (2005). Role of inflammatory mediators in angiogenesis. Curr Drug Targets 4, 3–8.
Nourshargh S, Hordijk PL, Sixt M (2010). Breaching multiple barriers: leukocyte motility through venular walls and the interstitium. Nat Rev Mol Cell Biol 11, 366–378.
Pan Q *et al*. (2007). Blocking neuropilin-1 function has an additive effect with anti-VEGF to inhibit tumor growth. Cancer Cell 11, 53–67.
Panne D, Maniatis T, Harrison SC (2004). Crystal structure of ATF-2/c-Jun and IRF-3 bound to the interferon-beta enhancer. EMBO J 23, 4384–4393.
Plotnikov A, Zehorai E, Procaccia S, Seger R (2011). The MAPK cascades: signaling components, nuclear roles and mechanisms of nuclear translocation. Biochim Biophys Acta 1813, 1619–1633.
Reglero-Real N, Marcos-Ramiro B, Millan J (2012). Endothelial membrane reorganization during leukocyte extravasation. Cell Mol Life Sci 69, 3079–3099.
Reimold AM, Kim J, Finberg R, Glimcher LH (2001). Decreased immediate inflammatory gene induction in activating transcription factor-2 mutant mice. Int Immunol 13, 241–248.
Rivera CG, Mellberg S, Claesson-Welsh L, Bader JS, Popel AS (2011). Analysis of VEGF–a regulated gene expression in endothelial cells to identify genes linked to angiogenesis. PLoS One 6, e24887.
Salameh A, Galvagni F, Anselmi F, De Clemente C, Orlandini M, Oliviero S (2010). Growth factor stimulation induces cell survival by c-Jun. ATF2-dependent activation of Bcl-XL. J Biol Chem 285, 23096–23104.
Schweighofer B, Testori J, Sturtzel C, Sattler S, Mayer H, Wagner O, Bilban M, Hofer E (2009). The VEGF-induced transcriptional response comprises gene clusters at the crossroad of angiogenesis and inflammation. Thromb Haemost 102, 544–554.
Seko Y, Takahashi N, Tobe K, Ueki K, Kadowaki T, Yazaki Y (1998). Vascular endothelial growth factor (VEGF) activates Raf-1, mitogen-activated protein (MAP) kinases, and S6 kinase (p90rsk) in cultured rat cardiac myocytes. J Cell Physiol 175, 239–246.
Shalaby F, Rossant J, Yamaguchi TP, Gertsenstein M, Wu XF, Breitman ML, Schuh AC (1995). Failure of blood-island formation and vasculogenesis in Flk-1-deficient mice. Nature 376, 62–66.
Sixt M, Bauer M, Lammermann T, Fassler R (2006). Beta1 integrins: zip codes and signaling relay for blood cells. Curr Opin Cell Biol 18, 482–490.
Stannard AK, Khurana R, Evans IM, Sofra V, Holmes DI, Zachary I (2007). Vascular endothelial growth factor synergistically enhances induction of E-selectin by tumor necrosis factor-alpha. Arterioscler Thromb Vasc Biol 27, 494–502.
Takahashi T, Yamaguchi S, Chida K, Shibuya M (2001). A single autophosphorylation site on KDR/Flk-1 is essential for VEGF-A-dependent activation of PLC-gamma and DNA synthesis in vascular endothelial cells. EMBO J 20, 2768–2778.
Testori J *et al*. (2011). The VEGF-regulated transcription factor HLX controls the expression of guidance cues and negatively regulates sprouting of endothelial cells. Blood 117, 2735–2744.
Usui T *et al*. (2004). VEGF164(165) as the pathological isoform: differential leukocyte and endothelial responses through VEGFR1 and VEGFR2. Invest Ophthalmol Vis Sci 45, 368–374.
Weber C (1996). Involvement of tyrosine phosphorylation in endothelial adhesion molecule induction. Immunol Res 15, 30–37.
Xu D, Fuster MM, Lawrence R, Esko JD (2011). Heparan sulfate regulates $VEGF_{165}$- and $VEGF_{121}$-mediated vascular hyperpermeability. J Biol Chem 286, 737–745.
Zhang Y, Furumura M, Morita E (2008). Distinct signaling pathways confer different vascular responses to VEGF 121 and VEGF 165. Growth Factors 26, 125–131.
Zhang HT, Scott PA, Morbidelli L, Peak S, Moore J, Turley H, Harris AL, Ziche M, Bicknell R (2000). The 121 amino acid isoform of vascular endothelial growth factor is more strongly tumorigenic than other splice variants in vivo. Br J Cancer 83, 63–68.